Preparative Oxidation of Organic Compounds in Microemulsions with Singlet Oxygen Generated Chemically by the Sodium Molybdate/Hydrogen Peroxide System[1]

Jean-Marie Aubry* and Sabine Bouttemy

Contribution from the "Equipe de Recherches sur les Radicaux Libres et l'Oxygène Singulet", CNRS URA 351, Faculté de Pharmacie de Lille, B.P. 83, F-59006 Lille Cedex, France

Received December 23, 1996[⊗]

Abstract: A reverse (water in oil) microemulsion has been designed to oxidize hydrophobic organic substrates with singlet oxygen ($^1O_2$, $^1\Delta_g$) generated from the disproportionation of hydrogen peroxide catalyzed by molybdate ions. The microemulsion was prepared by mixing methylene chloride, sodium dodecylsulfate, *n*-butanol, and aqueous molybdate. Flash photolysis studies have shown that in such media singlet oxygen exhibits a similar kinetic behavior that under homogeneous conditions ($\tau_\Delta \approx 42$ μs). Various typical organic substrates have been oxidized on the preparative scale with this chemically generated singlet oxygen, and the expected oxidation products have been isolated in high yields.

Introduction

Much work has been devoted to the chemistry and the biochemistry of singlet oxygen ($^1O_2$ ($^1\Delta_g$)) since the discovery, in the 1960s, of its involvement in the photodynamic effect, in the photooxygenation of organic compounds, and in the photodegradation of some polymers.[4] In contrast to ground state molecular oxygen, $^1O_2$ has found considerable synthetic utility since it can undergo selective reactions with a wide variety of electron-rich molecules such as olefins,[3] conjugated dienes, polycyclic aromatic hydrocarbons, phenols, sulfides, and heterocycles.[5]

This highly reactive oxidant is usually generated by photosensitization. This method is very versatile because it can be conducted in a wide range of solvents and at low temperature if unstable oxidized products have to be prepared. However, it requires photochemical reactors which are not always available in research laboratories or industrial plants; therefore, it has found very few industrial applications.[6]

On the contrary, chemical sources of $^1O_2$, involving readily available oxidants such as H_2O_2, could be attractive alternatives to the usual photochemical method. The most celebrated one involves the oxidation of H_2O_2 by ClO$^-$. It releases $^1O_2$ quickly and quantitatively according to eq 1:[7]

$$ClO^- + H_2O_2 \rightarrow H_2O + Cl^- + {}^1O_2 \ (100\%) \qquad (1)$$

Unfortunately, the high oxidizing power of ClO$^-$ leads to side reactions with substrates. On the other hand, a significant fraction of $^1O_2$ is lost through bubbles. This reaction has, thus, received few applications in organic synthesis, but it has found to be a very efficient generator of the gaseous $^1O_2$ required by the powerful chemical iodine laser.[8]

A milder chemical generator of $^1O_2$ has been discovered recently.[9] It involves the disproportionation of H_2O_2 catalyzed by MoO$_4^{2-}$. All of the oxygen produced is also in a singlet state but the intermediate peroxomolybdates are less reactive than ClO$^-$ (eq 2).

$$2H_2O_2 \xrightarrow{\text{MoO}_4^{2-}} 2H_2O + {}^1O_2 \ (100\%) \qquad (2)$$
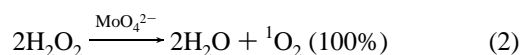
This reaction proceeds efficiently only in pure water and in aqueous MeOH or EtOH. Therefore, only organic substrates with some hydrophilicity and/or of low molecular weight can be oxidized on the preparative scale with this system.[10] One reaction medium used to overcome this solubility problem are the two-phase conditions described by McKeown and Waters[11] in which the acceptor is dissolved in chlorobenzene while the chemical generation of $^1O_2$ takes place in the aqueous layer. However, most of the $^1O_2$ is wasted through the deactivation by water molecules, since the mean travel distance of $^1O_2$ in water is only about 200 nm. A large excess of H_2O_2 is thus required to bring about appreciable conversion. In contrast, we show in the present work that a submicroscopic biphasic system

⊗ Abstract published in *Advance ACS Abstracts,* May 15, 1997.

(1) This paper is the 6th of a series about "Chemical sources of singlet oxygen". For the 5th paper, see: ref 2.

(2) Pierlot, C.; Hajjam, S.; Barthelemy, C.; Aubry, J. M. *J. Photochem. Photobiol., B* **1996**, *36*, 31−39.

(3) Prein, M.; Adam, W. *Angew. Chem., Int. Ed. Engl.* **1996**, *35*, 447−494.

(4) (a) Frimer, A. A. *Singlet Oxygen*; CRC Press: Boca Raton, FL, 1985; Vols. I−IV. (b) Ranby, B.; Rabek, J. F. *Singlet Oxygen*; J. Wiley and Sons: New York, 1975. (c) Wasserman, H. H.; Murray, R. W. *Singlet Oxygen*; Academic Press: New York, 1979; Vol. 40.

(5) (a) Wasserman, H. H.; Ives, J. L. *Tetrahedron* **1981**, *37*, 1825−1852. (b) Ohloff, G. *Pure Appl. Chem.* **1975**, *43*, 481−501.

(6) Gollnick, K. *Chim. Ind.* **1982**, *64*, 156−166.

(7) Khan, A. U.; Kasha, M. J. *J. Chem. Phys.* **1963**, *39*, 2105−2106. (b) Held, A. M.; Halko, D. J.; Hurst, J. K. *J. Am. Chem. Soc.* **1978**, *100*, 5732−5740.

(8) McDermott, W. E.; Pchelkin, N. R.; Benard, D. J.; Bousek, R. R. *Appl. Phys. Lett.* **1978**, *32*, 469−470.

(9) (a) Aubry, J. M. *J. Am. Chem. Soc.* **1985**, *107*, 5844−5849. (b) Aubry, J. M.; Cazin, B. *Inorg. Chem.* **1988**, *27*, 2013−2014. (c) Böhme, K.; Brauer, H. D. *Inorg. Chem.* **1992**, *31*, 3468−3471. (d) Niu, Q. J.; Foote, C. S. *Inorg. Chem.* **1992**, *31*, 3472−3476. (e) Nardello, V.; Marko, J.; Vermeersch, G.; Aubry, J. M. *Inorg. Chem.* **1995**, *34*, 4950−4957.

(10) (a) Aubry, J. M.; Cazin, B.; Duprat, F. *J. Org. Chem.* **1989**, *54*, 726−728. (b) Nardello, V.; Bouttemy, S.; Aubry, J. M. *J. Mol. Catal.* **1997**, *117*, 439−447.

(11) McKeown, E.; Waters, W. A. *J. Chem. Soc. B* **1966**, 1040−1046.

Preparative Oxidation of Organic Compounds

J. Am. Chem. Soc., Vol. 119, No. 23, 1997 5287

(microemulsion) is suitable for the chemical formation of $^1O_2$ and the oxidation of highly hydrophobic substrates on the preparative scale with a minimum loss of $^1O_2$.

Experimental Section

(A) Chemicals. Sodium molybdate dihydrate (99%), 5,6,11,12-tetraphenylnaphthacene (rubrene, Rub, **1**, 98%), 9,10-diphenylan-thracene (DPA, **2**, 98%), 1,3-diphenylisobenzofuran (DPBF, **3**, 97%), tetraphenylcyclopentadienone (tetracyclone, TCP, **4**, 98%), α-terpinene (Terp, **5**, 98%), β-citronellol (Citro, **7**, 95%), dibenzyl sulfide (DBS, **9**, 98%), diphenyl sulfide (DPS, **10**, 98%), 5,10,15,20-tetraphenyl-21*H*,-23*H*-porphine (TPP, 98%), and 5,10,15,20-tetraphenyl-21*H*,23*H*-por-phine-*p,p′,p″,p″*-tetrasulfonic acid, tetrasodium salt dodecahydrate (TPPS, 98%), were purchased from Aldrich Chemie and used as received. 2-Methyl-5-*tert*-butylthiophenol (**8**, 99%) was a generous gift of Hoechst France. Adamantylideneadamantane[12] (Ada, **6**) was prepared according to known procedures. Methylene chloride (Nor-mapur), butanol (Normapur), methanol (HPLC Grade), sodium dode-cylsulfate (SDS, 98%), and hydrogen peroxide (50%, Rectapur) were obtained from Prolabo. Deuteriated chloroform and deuterium oxide (99.9%) were acquired from CEA (Commissariat à l'Energie Atomique, Saclay, France).

(B) Instrumentation. HPLC. High-performance liquid chroma-tography analyses was carried out with a Gilson pump model 303 by using a 25 cm column packed with Spherisorb RP18-5 ODS. A mixture of H_2O and CH_3OH was used as eluent, and UV detection was performed with a variable-wavelength monitor (Gilson Holochrom H/MD).

Flash Photolysis. (Laboratoire de Biophysique, Museum National d'Histoire Naturelle, Paris.) The photosensitized production of $^1O_2$ was carried out by energy transfer from a photosensitizer (TPP or TPPS) to $^3O_2$. A 2 mL sample of an air-saturated microemulsion was irradiated with a short (6 ns) flash of light at 532 nm, emitted by a Nd-Yag laser. Infrared phosphorescence of singlet oxygen at 1270 nm was detected perpendicularly with a Ge photodiode (Judson J16), and the signal was recorded with an oscilloscope (Tektronix 556) and analyzed according to a first-order decay. The flash photolysis apparatus[13] and the detection system[14] have been previously described in detail.

^1H and ^{13}C NMR. (Laboratoire d'Applications RMN, Université de Lille II.) Spectra were recorded in $CDCl_3$ at 300 MHz for the ^1H and at 75.46 MHz for the ^{13}C by using a Bruker AC 300P FT-spectrometer. All chemical shifts are relative to the TMS signal (δ = 0 ppm) as reference.

(C) Procedures. Pseudoternary Phase Diagrams. The samples (12.5 g) were prepared in capped glass vials (50 mL) by introducing sequentially the surfactant (SDS), the cosurfactant (*n*-BuOH), and the organic solvent, (methylene chloride). The slurry obtained was maintained at a constant (20 ± 0.1 °C) temperature and titrated with 0.2 mL fractions of an aqueous sodium molybdate solution. After each addition, the samples were vigorously stirred, allowed to settle, and observed. It is the spontaneous conversion of the turbid emulsion into a clear, single-phase medium that indicates the beginning of the microemulsion region. Whereas the appearance of a persistent cloudy aspect leading to a phase separation after settling delimits the end of the microemulsion domain.

Microemulsions A−J. The microemulsion A was prepared at room temperature by adding dropwise an aqueous solution of sodium molybdate (1.15 g in 6 mL of water) to a magnetically stirred slurry of sodium dodecylsulfate (9.5 g), *n*-butanol (9.5 g), and methylene chloride (75 g). The transparent, mobile, isotropic medium obtained after 5 min of mixing can be kept unchanged in a capped flask for several weeks. Other microemulsions were prepared by applying the same procedure for the formulations reported in Table 1.

(12) (a) McMurry, J. E.; Flemming, M. P. *J. Am. Chem. Soc.* **1974**, *96*, 4708−4709. (b) Schaap, A. P.; Faler, G. R. *J. Org. Chem.* **1973**, *38*, 3061−3062.
(13) Vever-Bizet, C.; Dellinger, M.; Brault, D.; Rougee, M.; Bensasson, R. V. *Photochem. Photobiol.* **1989**, *50*, 321−325.
(14) Rodgers, M. A. J.; Snowden, P. T. *J. Am. Chem. Soc.* **1982**, *104*, 5541−5543.

Table 1. Formulations of Microemulsions on a Weight Basis

micro-emulsion	molybdate (mmol/kg)	water (%)	SDS (%)	butanol (%)	CH_2Cl_2 (%)	τ_Δ (μs)[a]		
						exp	hom	het
A	48	6.0	9.5	9.5	75.0	40.2		
B	5	5.0	7.7	15.3	72.0	42.4		
C		2.2	6.5	12.9	78.4	45.0	34.7	42.2
D		8.3	7.3	14.6	69.8	37.7	22.0	34.4
E		13.9	8.6	17.3	60.2	30.1	16.5	28.4
F		21.0	9.6	19.3	50.1	23.9	12.9	23.7
G		30.0	9.9	19.8	40.3	20.1	10.3	19.8
H		39.9	9.9	20.0	30.2	16.2	8.6	16.5
I		49.9	9.6	19.4	21.1	13.2	7.4	13.9

[a] Lifetimes of $^1O_2$ (τ_Δ) measured (exp) or calculated by considering the mixture as a homogeneous medium (hom) or a microheterogeneous system (het).

Oxidation of 9,10-Diphenylanthracene (2). A solution of 1.0 g (3.0 mmol) of **2** in the microemulsion B (50 g) was treated with 60 μL (1.0 mmol) of 50% H_2O_2. The red-brown solution was stirred at room temperature for 13 min until the color faded to gold-yellow. Nineteen other fractions of 60 μL of H_2O_2 were allowed to react in the same way, and the reaction was monitored by HPLC. Thus, after 4 h, **2** was completely oxidized. The solvents (methylene chloride, butanol, and water) were rotary evaporated at 40 °C in vacuum. The semisolid residue was stirred vigorously with 100 mL of methylene chloride for 30 min. The suspension was filtered by suction through a sintered-glass funnel to recover the solid sodium molybdate and sodium dodecylsulfate. The filtrate was rotary evaporated at 20 °C in vacuum, and the yellowish residue was washed successively with water (2 × 20 mL), methanol (2 × 20 mL), and ether (2 × 20 mL) giving 0.97 g (89%) of pure endoperoxide as crystalline colorless solid.
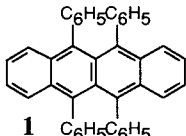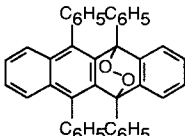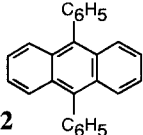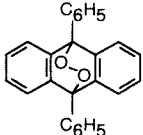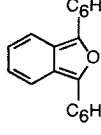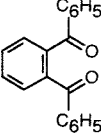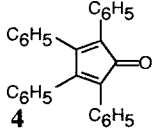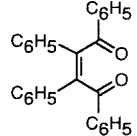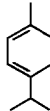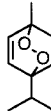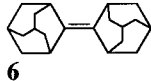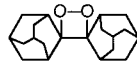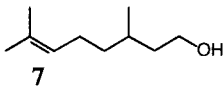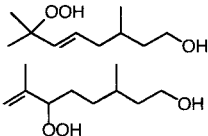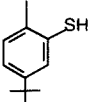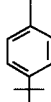
Oxidation of Other Substrates. The moderately soluble substrates **1−4** and **6** were oxidized according to the same procedure in the microemulsion B, whereas the microemulsion A was preferred for the highly soluble (**5** and **7**) and poorly reactive (**8−10**) substrates. To achieve a maximum rate for $^1O_2$ generation, H_2O_2 was added by fractions, each of them containing about 4 equiv of H_2O_2 with respect to MoO_4^{2-}. The fading of the red-brown to the gold-yellow color was the signal for an additional fraction of H_2O_2. The cumulative amounts of H_2O_2 consumed, the reaction times, and the yields are reported in Table 2. The products do not require further purification except ascaridol that was distilled (bp$_3$ = 77−78 °C). All the ^1H and ^{13}C NMR spectra were in agreement with the published spectra or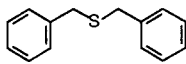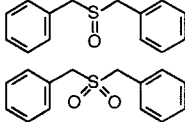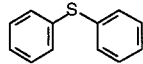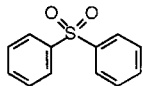 with those of authentic samples prepared by tetraphenylporphine-sensitized photooxygenation.[15] Control experiments without either H_2O_2 or MoO_4^{2-} did not lead to any consumption of the substrates. The unknown sulfonate obtained from the thiophenol **8** exhibits the following spectral data: ^1H NMR (D_2O) δ 1.34 (s, 9H, -C(C*H*$_3$)$_3$), 2.63 (s, 3H, Ar-C*H*$_3$), 8.05 (d, 1H, -C-(SO$_3$H)=C*H*), 7.37 (d, 1H, -C*H*=C-(CH$_3$)-), 7.6 (dd, 1H, -C*H*=C-C(CH$_3$)$_3$); ^{13}C NMR (D_2O) δ 143.14 (-C=*C*(SO$_3$H), 152.45 (-C=*C*(C(CH$_3$)$_3$)-), 136.01 (-C=*C*(CH$_3$)-), 134.89 (-*C*=C(CH$_3$)-), 126.55 (-*C*=C(SO$_3$H)-), 131.45 (-*C*=C-C(CH$_3$)$_3$), 36.82 (*C*(CH$_3$)$_3$), 33.30 (-C(*C*H$_3$)$_3$), 21.88 (*C*H$_3$-C=C-).

Results

Pseudoternary Phase Diagrams. The microemulsion region of the water/SDS/butanol/methylene chloride system delimits a volume included in a quaternary phase diagram. The boundaries of this volume were determined from pseudoternary phase diagrams obtained at 20 °C by maintaining the ratio of butanol/SDS at a constant value and titration with aqueous

(15) (a) Dufraisse, C. *Bull. Soc. Chim. Fr.* **1936**, *182*, 1584−1587. (b) Rigaudy, J.; Scribe, P.; Breliere, C. *Tetrahedron* **1981**, *37*, 2585−2593. (c) Dufraisse, C.; Ecary, S. *Compt. Rend.* **1946**, *223*, 735−773. (d) Bikales, N. M.; Becker, E. I. *J. Org. Chem.* **1956**, *21*, 1405−1407. (e) Schenck, G. O.; Ziegler, K. *Naturwissenschaften* **1945**, *32*, 157. (f) Wieringa, J. H.; Strating, J.; Wynberg, H.; Adam, W. *Tetrahedron Lett.* **1972**, 169−172. (g) Ohloff, G.; Lienhard, B. *Helv. Chim. Acta* **1965**, *48*, 182−189. (h) Jongsma, S. J.; Cornelisse, J. *Tetrahedron Lett.* **1981**, 2919−2922. (i) Koch, E. *Tetrahedron* **1968**, *24*, 6295−6318. (j) Liang, J. J.; Gu, M. L.; Kacher, M. L.; Foote, C. S. *J. Am. Chem. Soc.* **1983**, *105*, 4717−4721.

Table 2. Oxidation of a Variety of Typical Organic Substrates in Reverse Microemulsions by the Oxidizing System H_2O_2/MoO_4^{2-} at 25 °C

Substrate	$\log(k_r+k_q)$[a]	$\dfrac{k_r}{k_r + k_q}$	[Substrate] mmol·kg^{-1}	[H_2O_2] mmol·kg^{-1}	Time h	Product	Yield[c] %
1	7.6	1.0[a]	10[B]	30	0.5		98
2	6.2	0.34[a]	60[B]	400	2.0		89
3	8.9	1.0[a]	100[B]	300	1.5		91
4	8.4	0.30[a]	90[B]	700	3.5		78
5	8.0 / 7.6[b]	1.0[b]	490[A]	1100	1.0		70
6	5.9	0.4[b]	120[B]	1000	4.0		90
7	5.9 / 6.0[b]	0.87[b]	390[A]	1500	1.3		40 / 42
8	–	–	100[A]	700	2.0		88
9	6.8	0.4[b]	90[A]	540	1.6		48 / 48
10	4.9	0.85[b]	100[A]	10900	24.0		40

A and B: oxidations carried out in the microemulsions A and B, respectively. [a] Average value calculated from ref 16. [b] Our work. [c] Isolated after purification except for substrates **7**, **9**, and **10**, determined by ^1H NMR spectroscopy.

sodium molybdate at various concentrations. The diagrams corresponding to the ratios 1 and 2 are given in Figure 1.

Kinetic Behavior of Singlet Oxygen in Microemulsion. The photosensitized production of singlet oxygen ($^1\Delta_g$) and its different pathways of decay are presented in Scheme 1.[16]

The k_d is the pseudo-first-order rate constant of singlet oxygen

decay in the solvent, k_q and k_r are the bimolecular rate constants for the physical and the chemical quenching of singlet oxygen by a substrate S, and k_p is the first-order rate constant of phosphorescence decay. In solution, the nonradiative pathways

(16) Wilkinson, F.; Helman, W. P.; Ross, A. B. *J. Phys. Chem. Ref. Data* **1995**, *24*, 663−1021.
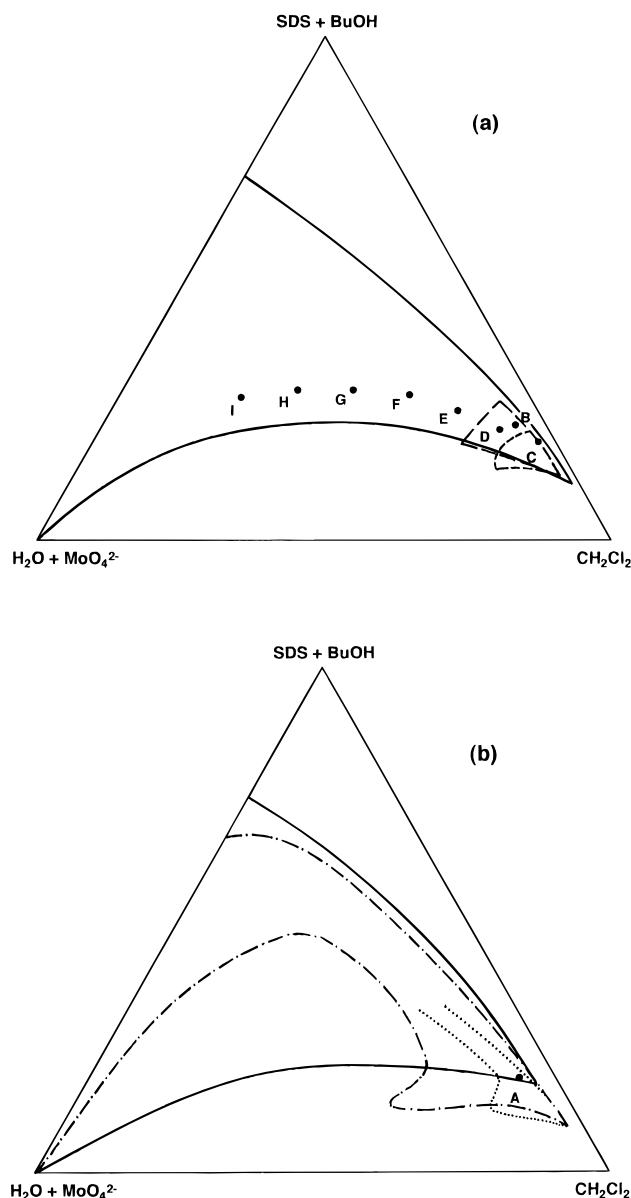
Figure 1. Microemulsion pseudoternary phase diagrams of the system water/SDS + butanol/methylene chloride. The aqueous phase contains sodium molybdate 0.0 M (—), 0.1 M (− − −), 0.2 M (- - -), 0.4 M (− · −), or 0.8 M (···). $T = 20.0$ °C, and weight ratio butanol/SDS is 2.0 (a) or 1.0 (b). Dots represent the microemulsions used for preparative purpose (A and B) or kinetic experiments (C to I).

Scheme 1

formation of $^1O_2$　　　　source of $^1O_2$ $\rightarrow$ $^1O_2$　(3)

quenching by microemulsion　$^1O_2$ + solvent $\xrightarrow{k_d}$ $^3O_2$　(4)

physical quenching　　　　$^1O_2$ + S $\xrightarrow{k_q}$ $^3O_2$ + S　(5)

chemical quenching　　　　$^1O_2$ + S $\xrightarrow{k_r}$ SO_2　(6)

phosphorescence　　　　　$^1O_2$ $\xrightarrow{k_p}$ $^3O_2$ + $h\nu$　(7)

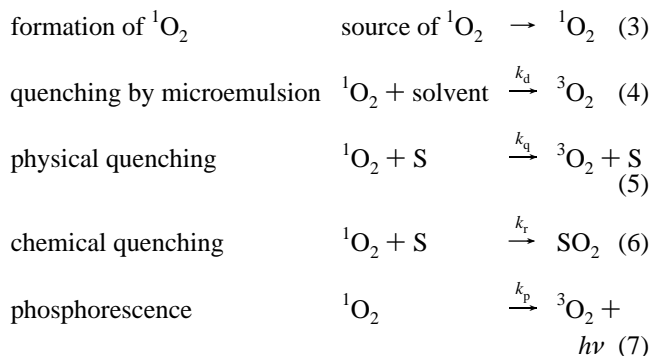(eqs 4−6) predominate the total deactivation process and the deactivation channel by phosphorescence (eq 7) may be neglected.[17] However, the detection of this luminescence is a very convenient method for monitoring the kinetics of singlet

oxygen. With this $^1O_2$ phosphorescence, we have measured the rate constants, k_d and $k_r + k_q$, by the laser flash photolysis technique.[18] The ratio $k_r/(k_r + k_q)$ was determined by submitting increasing concentrations of substrate to a given amount of $^1O_2$ generated from a chemical source of $^1O_2$.[19]

Flash Photolysis. In aerated microemulsion, after laser excitation of the photosensitizer, the production of singlet oxygen is completed in step 3 within less than 2 μs. Following this, singlet oxygen decays *via* reactions 4−6. This simple scheme assumes that $^1O_2$ behaves kinetically in microemulsions in the same way as in homogeneous media. In particular, the lifetime of $^1O_2$ should not depend on the location of the photosensitizer. In order to confirm this assumption, we have shown that the lifetime of $^1O_2$ measured in the microemulsion B is similar ($\tau_\Delta = 42.4$ μs) by using either a hydrophilic photosensitizer (TPPS), which is confined within the aqueous droplets or in the interfacial film, or a hydrophobic photosensitizer (TPP), which dissolves in the organic continuous phase.

Therefore, the current kinetic treatment may be applied to this system and the rate of $^1O_2$ decay may be expressed according to eq 8.[16]

$$-\frac{d[^1O_2]}{dt} = k_{obsd}[^1O_2] = \{k_d + (k_r + k_q)[S]\}[^1O_2] \quad (8)$$

Under our experimental conditions, as S is present in excess of the initial concentration of singlet oxygen $[^1O_2]_0$, the concentration of the substrate [S] is constant during the irradiation. Therefore, integration of eq 8 gives eq 9.

$$[^1O_2] = [^1O_2]_0 \exp -(k_{obsd}t) = [^1O_2]_0 \exp -\{k_d + (k_r + k_q)[S]\}t \quad (9)$$

The exponential decay of $^1O_2$ was monitored through its phosphorescence (eq 7). The values of $k_{obsd} = k_d + (k_r + k_q)$-[S] were derived from single-exponential fittings of the decay curves, and the overall bimolecular rate constant for quenching of $^1O_2$, $(k_r + k_q)$, was obtained by the Stern−Volmer kinetic analysis in which k_{obsd} is plotted *versus* the substrate concentration [S]. The value of $(k_r + k_q)$ is the slope of the straight line obtained, and k_d is its intercept with the y axis. Overall rate constants $(k_r + k_q)$ of α-terpinene (**5**) and β-citronellol (**8**) in the microemulsion A were found to be very similar to those reported in the literature under homogeneous conditions (Table 2).

The lifetime of $^1O_2$ ($\tau_\Delta = 1/k_d$) was determined in microemulsions with increasing amounts of water (C to I in Figure 1a). The experimental lifetimes are reported in Table 1 as a function of water concentration. All values fall between the lifetimes of $^1O_2$ in pure water (4.4 μs) and methylene chloride (97 μs).[16] τ_Δ shows little dependence on the molybdate concentration and on the ratio of butanol/SDS, but it decreases sharply when the amount of water increases.

Chemical Oxidation of α-Terpinene and β-Citronellol. Kinetic studies were performed in the microemulsion A with various concentrations of the substrate S to which sufficient hydrogen peroxide was added to oxidize approximately 50% of the substrate. Once generated by the reaction 2, singlet oxygen decays according to the physical quenching (eqs 4 and 5) and to the oxidation process (eq 6). Under stationary-state

(17) Schmidt, R.; Afshari, E. *Ber. Bunsen-Ges. Phys. Chem.* **1992**, *96*, 788−794.
(18) Aubry, J. M.; Mandard-Cazin, B.; Rougee, M.; Bensasson, R. V. *J. Am. Chem. Soc.* **1995**, *117*, 9159−9164.
(19) Caminade, A. M.; El Khatib, F.; Koenig, M.; Aubry, J. M. *Can. J. Chem.* **1985**, *63*, 3203−3209.

conditions ($d[^1O_2]/dt = 0$), and after integration between zero time and infinite time, we obtain the expression (eq 10) already demonstrated by Wilkinson et al.,[16] where the infinite time refers to the completion of the hydrogen peroxide disproportionation. The final concentration of the substrate $[S]_\infty$ is thus related to the cumulative amount of $^1O_2$ generated in the medium ($[^1O_2]_\infty = [H_2O_2]_0/2$) and to the physical and the chemical quenching rate constants k_q and k_r.

$$\frac{k_d}{k_r + k_q} \ln \frac{[S]_0}{[S]_\infty} + [S]_0 - [S]_\infty = \frac{k_r}{k_r + k_q}[^1O_2]_\infty \quad (10)$$

The ratio $\gamma = k_r/(k_r + k_q)$ expresses the contribution of the chemical quenching in the overall quenching. Whereas, $\beta = k_d/(k_r + k_q)$ is the Foote reactivity index that corresponds to the minimum concentration of substrate required so that the interaction of $^1O_2$ with the substrate (eqs 5 and 6) becomes predominant over the deactivation of $^1O_2$ by the microemulsion (eq 4).

A plot of $([S]_0 - [S]_\infty)/[^1O_2]_\infty$ *versus* $\{\ln([S]_0/[S]_\infty)\}/[^1O_2]_\infty$ gives a straight line with γ as intercept with the *y* axis.[19] This simple method has been applied to α-terpinene and β-citronellol leading to γ values of 1.0 and 0.87, respectively. The value of 1.0 found for α-terpinene implies that all of the singlet oxygen generated in the aqueous droplets is chemically trapped by the α-terpinene solubilized in the microemulsion A. Whereas, for β-citronellol, some physical quenching competes with the predominant chemical quenching.

Peroxidation of Organic Substrates on the Preparative Scale. Ten typical organic substrates which include the two olefins **6** and **7**, the two conjugated dienes **4** and **5**, the two polycyclic aromatic hydrocarbons **1** and **2**, the thiophenol **8**, the two sulfides **9** and **10**, and the heterocycle **3** were oxidized on the preparative scale to show the scope of this oxidizing system. These substrates represent four standard types of $^1O_2$ reactions, namely, the ene reaction, the [2 + 2] cycloaddition, the [4 + 2] cycloaddition, and the sulfide oxidation. The respective oxidation products were isolated in high yields (Table 2), and the catalyst (molybdate) and the surfactant (SDS) were recovered on workup.

The moderately soluble substrates **1−4** and **6** were preferably oxidized in the microemulsion B for which workup is easier because it contains a minimum amount of molybdate and SDS. For the highly soluble (**5** and **7**) and poorly reactive (**8−10**) substrates, the microemulsion A was preferred because higher amount of hydrogen peroxide can be solubilized without phase separation and because it contains a 10 times higher concentration of the molybdate catalyst. The hydrogen peroxide must be added in batches to favor the formation of the red-orange triperoxomolybdate $MoO(O_2)_3^{2-}$, the precursor of $^1O_2$, and to avoid the red-brown tetraperoxomolybdate $Mo(O_2)_4^{2-}$, which does not generate $^1O_2$.[9e] Thus, each fraction of hydrogen peroxide must not contain more than 4 equiv of hydrogen peroxide with respect to molybdate. While the disproportionation of hydrogen peroxide proceeds (eq 2), the red-orange color due to the triperoxomolybdate fades to gold-yellow when the diperoxomolybdate becomes the prevalent peroxomolybdate. This change of color is the visual endpoint for an additional batch of hydrogen peroxide.

The oxidation of the substrate S and the formation of the product SO₂ were monitored by HPLC. Each starting material could be completely oxidized without separation of the microemulsion, except the poorly reactive diphenyl sulfide which was converted to diphenyl sulfone up to only 40%, although a very large excess of $^1O_2$ was employed. The total amount of
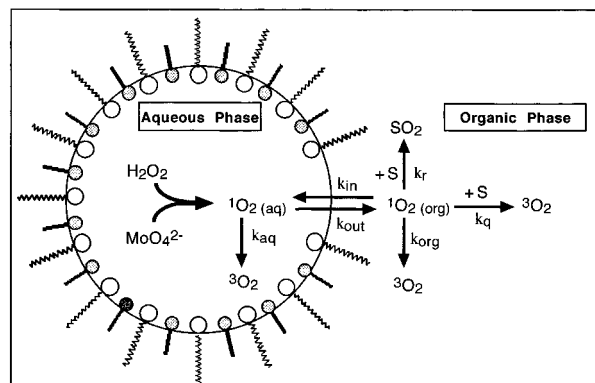
Figure 2. Schematic representation of the water-in-oil microemulsions used to oxidize organic substrates by the chemical source of singlet oxygen H_2O_2/MoO_4^{2-}.

hydrogen peroxide required to achieve complete oxidation, $[H_2O_2]$, depends strongly on the reactivity of the substrate. Thus, the ratio $[H_2O_2]_\infty/[S]_0$ varies between 2.2 and 109 and reflects the overall reactivity of the substrate and the relative contributions of the chemical (eq 6) and the physical (eq 5) quenching (Table 2).

Discussion

Phase Behavior of the Sodium Molybdate Microemulsion. A microemulsion, which consists of water, organic solvent (oil), surfactant, and in most cases cosurfactant, is defined as a transparent or translucent, thermodynamically stable, isotropic dispersion of two immiscible liquids with microdomains of one or both liquids stabilized by an interfacial film of surface-active molecules. Depending on the proportions of the constituents, three main types of structure can be distinguished: reverse micelles (W/O), direct micelles (O/W), or bicontinuous structures.[20] The water-in-oil microemulsions, which were mainly used in the present study, are described as roughly spherical water microdroplets coated by an interfacial film of SDS and butanol and dispersed in a continuous phase of methylene chloride (Figure 2).

One important feature of these media is their ability to dissolve simultaneously considerable amounts of hydrophilic compounds that are confined in aqueous droplets and nonpolar organic molecules that are localized in the continuous organic phase. Thus, hydrogen peroxide and sodium molybdate are compartmentalized in an aqueous microreactor, where they generate $^1O_2$ quantitatively according to eq 2. Since singlet oxygen is a small, uncharged molecule, it can diffuse freely through the charged interfacial region.[21] Moreover, the typical size of the microdroplets ($\sim$10 nm) is much smaller than the mean travel distance of $^1O_2$ in water ($\sim$200 nm). Therefore, despite the short lifetime of $^1O_2$ in water (4.4 μs), this species can diffuse before deactivation from the aqueous droplets to the methylene chloride phase, in which it reacts with the substrate. Thus, a very reactive substrate such as α-terpinene (**5**) traps almost all of the generated singlet oxygen.

During the peroxidation of organic substrates by the catalytic system H_2O_2/MoO_4^{2-}, seven components are present in the microemulsion: water, the surfactant (SDS), the cosurfactant

(20) (a) Mackay, R. A. *Adv. Colloid Interface Sci.* **1981**, *15*, 131−156. (b) Friberg, S. E.; Bothorel, P. *Microemulsions: structure and dynamics*; CRC Press: Boca Raton, FL, 1987. (c) Lattes, A. J. *J. Chim. Phys.* **1987**, *84*, 1061−1073. (d) Bourrel, M.; Schechter, R. S. *Microemulsions and related systems*; Surfactant Science Series; Dekker: New York, 1988; Vol. 60.

(21) Lee, P. C.; Rodgers, M. A. J. *J. Phys. Chem.* **1984**, *88*, 4385−4389.

(BuOH), the organic solvent (CH_2Cl_2), the substrate, the catalyst (Na_2MoO_4), and the oxidant (H_2O_2). The first four compounds (i.e., water, SDS, butanol, and methylene chloride) constitute the reaction medium itself, independent of the particular reaction that is carried out. The next two compounds, substrate and sodium molybdate, belong to the reactants that are dissolved in the microemulsion before the beginning of the reaction. The last reactant, hydrogen peroxide, is added in batches to the reaction medium. It generates the required $^1O_2$, but also some water as a side product derived both from the disproportionation and from the water of dilution of hydrogen peroxide.

Ideally, the microemulsion should be designed to meet the following requirements: (i) no phase separation during storage and during the oxidation reaction, (ii) high solubility of the three reactants (H_2O_2, MoO_4^{2-}, substrate), and (iii) simple recovery of the oxidized product, surfactant, and catalyst at the end of the reaction. Furthermore, none of the components of the microemulsion itself should react with hydrogen peroxide and molybdate or the intermediates derived therefrom (peroxo-molybdates and singlet oxygen). Therefore, methylene chloride was chosen as the oil because it is an excellent solvent for organic substrate, SDS was selected as surfactant because its strongly ionic feature allows its separation from the product, and butanol was taken as cosurfactant since it is relatively volatile. For this formulation, the workup at the end of the oxidation is straightforward. In most of the published work, this critical problem is either bypassed by analyzing the medium without separation[22] or lengthy extractions are carried out[23] and, in both cases, costly catalyst and surfactant are wasted. In our case, the microemulsion is simply rotary evaporated at 40 °C to remove of methylene chloride, water, and butanol to leave a pasty mixture of molybdate, SDS, and oxidized product. The nonpolar product is then selectively solubilized in methylene to recover the reusable surfactant and catalyst by filtration.

Another major concern with microemulsions is the stability problem when high concentrations of reactants are solubilized. The pseudoternary phase diagram of the system water/SDS + butanol/methylene chloride with a weight ratio of butanol/SDS = 2.0 (Figure 1a) exhibits a wide microemulsion domain, but when sodium molybdate is added, this domain is reduced drastically and disappears completely when the molybdate concentration in water is higher than 0.4 M. This phenomenon is due to the influence of the ionic force on the structure of the interfacial film. The sodium cations of sodium molybdate decrease the repulsion between the negatively charged head groups of SDS and, hence, favor the formation of reverse micelles. The interfacial film also becomes more rigid as a result of the compacting of the polar head groups, and the exchange rate of butanol between the interfacial layer, namely, the aqueous phase and the organic phase, is slower.[20,24]

The gradual addition of hydrogen peroxide during the reaction increases the ratio of water in the microemulsion. Therefore, since the initial formulation B lies next to the water-poor boundary of the microemulsion (Figure 1a), the composition shifts along the dilution line up to the biphasic domain. Phase separation occurs when 10% of water is added. It corresponds to the disproportionation of 1.7 M of 50% hydrogen peroxide and to the generation of a cumulative amount of 0.89 M of $^1O_2$.

Higher concentrations of molybdate ($[MoO_4^{2-}]_{aq} = 0.8$ M) and of hydrogen peroxide (3.4 M) can be solubilized in the microemulsion A, formulated with a ratio of butanol/SDS equal to 1.0 (Figure 1b). However, in this case, the residue obtained after the evaporation of the reaction medium contains higher amounts of molybdate and SDS and the recovery of the product is somewhat more tedious. Therefore, this microemulsion was used only for highly soluble or poorly reactive substrates that require the generation of a considerable amount of $^1O_2$ for complete oxidation of the substrate.

Kinetic Model

The kinetic behavior of $^1O_2$ in a homogeneous solution of the substrate S is properly described by eqs 3–6. Nevertheless, this set of reactions is insufficiently detailed to account for the behavior of $^1O_2$ in our microheterogeneous systems. The compartmentalization of aqueous microdroplets and the transfer processes of $^1O_2$ between aqueous and organic phases need to be accounted for. An adequate kinetic scheme related to that proposed by Rodgers et al. is depicted in Figure 2.[25] The validity of the model is based on the fact that the typical size of the aqueous microdroplets (~10 nm) is considerably smaller than the mean distance traveled by $^1O_2$ before deactivation by water molecules (~200 nm).[25h] When one $^1O_2$ molecule is chemically generated in an aqueous droplet, it can either be quenched by water and hydrophilic solutes with a rate constant (k_{aq}) or diffuse out of the droplet into the organic phase (k_{out}) of the substrate S. Once inside the continuous phase, the excited species can either (i) reenter the swollen micelle (k_{in}), (ii) decay to $^3O_2$ by physical quenching with the organic phase (k_{org}) or substrate (k_q), or (iii) react with the substrate S (k_r) to the oxidized product SO_2. This kinetic scheme can be simplified if it is assumed that the equilibration of $^1O_2$ between the two phases is rapid compared with the decay pathways (i.e., k_{out}, $k_{in} \gg k_{aq}$, k_{org}, $(k_r + k_q)[S]_{org}$). These conditions are fulfilled since $k_{aq} = 2.3 \times 10^5$ s^{-1} in pure water and $k_{org} = 1.0 \times 10^4$ s^{-1} in pure methylene chloride, whereas the rate constants by which $^1O_2$ enters into or exits from micellar aggregates have been reported to be not less than 10^7 s^{-1}.[25d] In agreement with this assumption, we have shown that the lifetime of $^1O_2$ in the microemulsion B ($\tau_\Delta = 42.4$ μs) is independent of the locality (water or methylene chloride) and of the hydrophilicity (TPPS or TPP) of the photosensitizer. Thus, an equilibrium is established for $^1O_2$ between the two phases and the rate constants k_{out} and k_{in} can be replaced by the equilibrium constant K (eq 11).

$$K = [^1O_2]_{aq}/[^1O_2]_{org} = k_{in}/k_{out} \qquad (11)$$

However, for high concentrations of substrate, the term $(k_r + k_q)[S]_{org}$ may dominate and the equilibrium condition is no longer valid. This case is kinetically simple since it corresponds to the situation for which all the generated singlet oxygen is scavenged by the substrate.

The kinetic scheme depicted in Figure 2 has been resolved by Lee and Rodgers[25d] under equilibrium conditions. We have adopted a similar approach except that a reactive substrate S is included in the model. Our aim was to express the "apparent" rate constants as a function of the composition of the micro-

(22) (a) Larpent, C.; Patin, H. *J. Mol. Catal.* **1992**, *72*, 315–329. (b) Menger, F. M.; Elrington, A. R. *J. Am. Chem. Soc.* **1991**, *113*, 9621–9624.

(23) Martin, C. A.; McCrann, P. M.; Angelos, G. H.; Jaeger, D. A. *Tetrahedron Lett.* **1982**, *23*, 4651–4654.

(24) Kahlweit, M.; Srey, R.; Schomächer, R.; Haase, D. *Langmuir* **1989**, *5*, 305–315.

(25) (a) Gorman, A. A.; Lovering, G.; Rodgers, M. A. J. *Photochem. Photobiol.* **1976**, *23*, 399–403. (b) Matheson, I. B. C.; Massoudi, R. *J. Am. Chem. Soc.* **1980**, *102*, 1942–1948. (c) Matheson, I. B. C.; Rodgers, M. A. J. *J. Phys. Chem.* **1982**, *86*, 884–887. (d) Lee, P. C.; Rodgers, M. A. J. *J. Phys. Chem.* **1983**, *87*, 4894–4898. (e) Rodgers, M. A. J.; Lee, P. C. *J. Phys. Chem.* **1984**, *88*, 3480-3484. (f) Racinet, H.; Jardon, P.; Gautron, R. *J. Chim. Phys.* **1988**, *85*, 971–977. (g) Lissi, E. A.; Encinas, M. V.; Lemp, E.; Rubio, M. A. *Chem. Rev.* **1993**, *93*, 699–723. (h) Lissi, E. A.; Rubio, M. A. *Pure Appl. Chem.* **1990**, *62*, 1503–1510.

emulsion and of the rate constants measured for each component in the homogeneous media.

The mean concentration of $^1O_2$ in the entire volume, namely, $[^1O_2]$, can be expressed according to eq 12 where f and $(1 - f)$ are the volume fractions of aqueous and organic phases, respectively.

$$[^1O_2] = f[^1O_2]_{aq} + (1 - f)[^1O_2]_{org} \quad (12)$$

The time derivative of eq 12 leads to eq 13.

$$\frac{d[^1O_2]}{dt} = f\frac{d[^1O_2]_{aq}}{dt} + (1 - f)\frac{d[^1O_2]_{org}}{dt} \quad (13)$$

The individual rate equations which govern the concentration of $^1O_2$ in each phase are given by eqs 14 and 15

$$\frac{d[^1O_2]_{aq}}{dt} = {}^1/_2\frac{d[H_2O_2]_{aq}}{dt} + k_{in}[^1O_2]_{org} - (k_{out} + k_{aq})[^1O_2]_{aq} \quad (14)$$

$$\frac{d[^1O_2]_{org}}{dt} = k_{out}[^1O_2]_{aq} - \{k_{in} + k_{org} + (k_r + k_q)[S]_{org}\}[^1O_2]_{org} \quad (15)$$

where $d[H_2O_2]_{aq}/dt$ is the rate of H_2O_2 disproportionation equal to twice the rate of $^1O_2$ generation. By substituting eqs 12, 14, and 15 into eq 13 and assuming the fast equilibrium condition (eq 11), we obtain eq 16.

$$\frac{d[^1O_2]}{dt} = f{}^1/_2\frac{d[H_2O_2]_{aq}}{dt} - \left\{\frac{[fk_{aq}K + (1 - f)k_{org}] + (k_r + k_q)(1 - f)[S]_{org}}{fK + 1 - f}\right\}[^1O_2] \quad (16)$$

This expression reduces to eq 17 by using the mean concentrations $[H_2O_2] = f[H_2O_2]_{aq}$ and $[S] = (1 - f)[S]_{org}$ referring to the bulk volume instead of the local concentrations.

$$\frac{d[^1O_2]}{dt} = {}^1/_2\frac{d[H_2O_2]}{dt} - \left\{\frac{[fk_{aq}K + (1 - f)k_{org}] + (k_r + k_q)[S]}{fK + 1 - f}\right\}[^1O_2] \quad (17)$$

From a macroscopic point of view, this microemulsion may be considered a homogeneous mixture characterized by the apparent rate constants k_d^{app}, k_q^{app}, and k_r^{app} referring respectively to the deactivation of $^1O_2$ by the microemulsion and to the physical and the chemical quenching of $^1O_2$ by the substrate S. Hence, the rate of the $^1O_2$ reaction may be expressed by the simple relation in eq 18.[16]

$$\frac{d[^1O_2]}{dt} = {}^1/_2\frac{d[H_2O_2]}{dt} - \{k_d^{app} + (k_r^{app} + k_q^{app})[S]\}[^1O_2] \quad (18)$$

Comparison of eqs 17 and 18 leads to eqs 19−21.

$$k_d^{app} = \frac{fk_{aq}K + (1 - f)k_{org}}{fK + 1 - f} \quad (19)$$

$$k_r^{app} = \frac{k_r}{fK + 1 - f} \quad (20)$$

$$k_q^{app} = \frac{k_q}{fK + 1 - f} \quad (21)$$

Table 3. Bimolecular Physical Quenching Rate Constants for the Constituents of Microemulsions

constituent	H_2O	CH_2Cl_2	n-BuOH	SDS	$Na_2MoO_4 \cdot 2H_2O$
k_q^A (M^{-1} s^{-1})	4100	640	5240	16900	13500

In this kinetic analysis, the microemulsion is considered as a dispersion of aqueous microdroplets separated from the organic continuous phase by a clear-cut boundary. Clearly, such a simplified scheme is far from reality. In particular, the boundary between the aqueous and the organic phase is better depicted as a saturated layer of a mixture of surfactant (SDS) and cosurfactant (butanol).[20] Nevertheless, this model has been adequate to account for our experimental results. For the calculations, we have included all of the organic components in the "organic phase" (methylene chloride, SDS, substrate) and the inorganic ones in the "aqueous phase" (water, sodium molybdate). Butanol is the most critical component, since it is present simultaneously in the aqueous droplets, in the continuous organic phase, and in the interfacial film. As a rough approximation, it was assumed that butanol distributes between the organic and the aqueous phase with the same ratio as that in a biphasic system of pure methylene chloride and water ($[BuOH]_{org}/[BuOH]_{aq} = 5.0$).

In a homogeneous mixture free from substrate, the first-order rate constant of $^1O_2$ deactivation, k_d^{mixt}, is correctly predicted by the simple additive expression in eq 22[25g]

$$k_d^{mixt} = 1/\tau_\Delta^{mixt} = \sum k_q^A[A] \quad (22)$$

where $[A]$ is the concentration of the constituent A calculated for the entire volume of the microemulsion and k_q^A is the bimolecular rate constant for the quenching of $^1O_2$ by A.

The second-order quenching rate constants k_q^A of the solutes sodium molybdate and SDS were measured in deuterated water by flash photolysis, whereas the second-order quenching rate constants of the solvents were readily calculated from the reported first-order rate constants, $k_q^A = k_d^A/[A]$ (Table 3).[16]

In a first approach, the predicted $^1O_2$ lifetimes (i.e., τ_Δ) in the various microemulsions were calculated from the known compositions (Table 1) and from eq 22 by assuming that all the constituents are homogeneously distributed in the mixture. The values obtained (Table 1, column "hom") are in all cases much lower than the experimental values (column "exp"). In particular, the predicted lifetime is almost twice as short as the measured lifetime for the microemulsion H which is expected to have a bicontinuous structure.

In a second approach, the measured $^1O_2$ lifetimes have been rationalized from the kinetic model proposed by Rodgers et al. who take into account the microheterogeneity of the system.[25] In this model, $^1O_2$ distributes itself between the aqueous and the organic phases during its lifetime according to the equilibrium constant K. The data were analyzed with eq 19 that can be rearranged into eq 23, where $k_{org} = 640[CH_2Cl_2]_{org} + 5240[BuOH]_{org} + 16900[SDS]_{org}$ and $k_{aq} = 5240[BuOH]_{aq} + 4100[H_2O]_{aq} + 13500[MoO_4^{2-}]_{aq}$.

$$\frac{k_d^{app} - k_{org}}{k_{aq} - k_d^{app}} = \frac{f}{1 - f}K \quad (23)$$

A plot of $(k_d^{app} - k_{org})/(k_{aq} - k_d^{app})$ *versus* $f/(1 - f)$ is linear (Figure 3) with an intercept close to the origin as expected from eq 23, and the slope is $K = 0.24$. Hence, $^1O_2$ is 4.2 times more
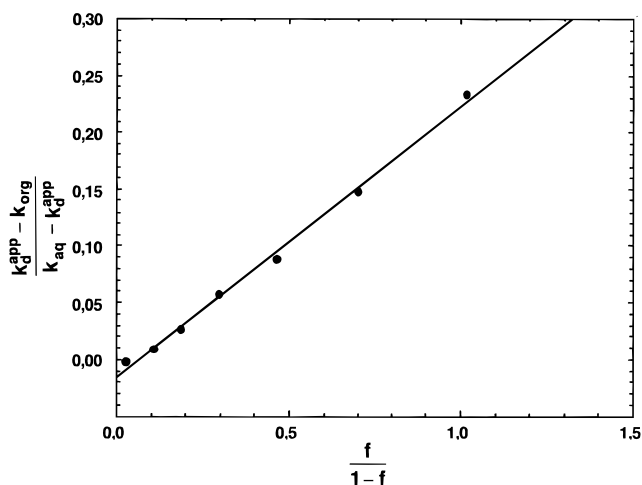
Figure 3. Plots of $(k_d^{app} - k_{org})/(k_{aq} - k_d^{app})$ as function of $f/(1 - f)$ in $CH_2Cl_2/BuOH/SDS/H_2O$ microemulsions for seven different water concentrations.

soluble in the organic phase than in the aqueous droplets, whereas a value of 10 was expected from the respective solubilities of ground state oxygen in pure methylene chloride and water. This discrepancy does not arise from different solubility of ground state and singlet state oxygen since Lee and Rodgers have found a value of K equal to 0.11 for the distribution of $^1O_2$ in the microheterogeneous system water AOT (sodium bis(2-ethylhexyl)sulfosuccinate) heptane.[25d] The higher value found for K with our microemulsion is better explained by the presence of some butanol in the aqueous phase which increases the oxygen solubility in the resulting mixed solvent compared with the solubility in neat water.

Chemical Peroxidation of Organic Substrates

Our aim was to use the system H_2O_2/MoO_4^{2-} to oxidize, on a preparative scale and within a reasonable time, various typical organic substrates dissolved in microemulsion. The preferred formulation of the microemulsion should contain a maximum amount of methylene chloride and molybdate and a minimum amount of surfactant and cosurfactant in order to dissolve high concentrations of substrate and to generate a high flux of $^1O_2$. Hence, the best microemulsions are localized in the oil-rich domain of the pseudoternary diagrams shown on Figure 1. Furthermore, in this region the lifetime of $^1O_2$ is the longest (formulations A–C of Table 1).

In practice, the extent of peroxidation is considered complete when more than 99% of the starting material is consumed. However, this goal may be achieved only if a sufficient amount of $^1O_2$ can be generated from the disproportionation of H_2O_2 without separation of the microemulsion. The reactivity of a given substrate toward $^1O_2$ can be depicted by the chemical and the physical quenching rate constants k_r and k_q. The maximum concentration of a given substrate S that can be completely oxidized can be estimated from eq 10. It relates the cumulative amount of $^1O_2$, $[^1O_2]_\infty$, with the starting ($[S]_0$) and final ($[S]_\infty$) concentrations of the substrate S and k_r^{app} and k_q^{app} are the apparent chemical and physical quenching rate constants of S toward $^1O_2$. These constants can be calculated from eqs 20 and 21 and from the published values of the rate constant measured in pure solvents (Table 2).

Most of the oxidations were carried out in the oil-rich microemulsion B, which dissolves organic substrates almost as efficiently as pure methylene chloride. If V_0 is the initial volume of the microemulsion and V is the volume of added hydrogen peroxide at the concentration α, the ratio V/V_0 must be less than
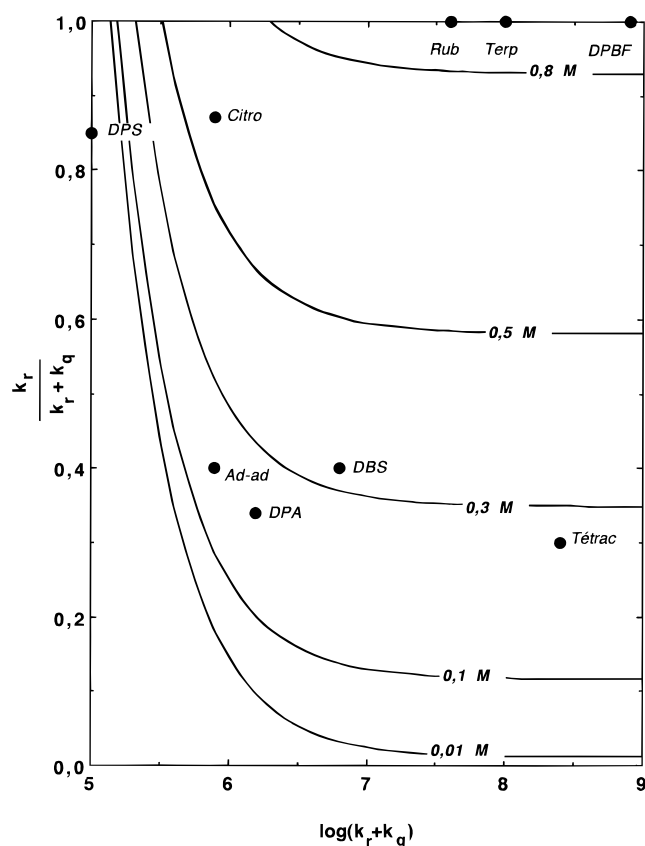
Figure 4. Estimated concentration of the substrate for its complete oxidation in the microemulsion B as a function of its overall reactivity $(k_r + k_q)$ and of the fraction of chemical quenching $k_r/(k_r + k_q)$.

0.1 to avoid phase separation. Therefore, the maximum cumulative amount of $^1O_2$ that can be generated in a volume V of the microemulsion B by disproportionation of H_2O_2 is $[^1O_2]_\infty = \alpha V/2V_0$. Moreover, for 99% conversion of the substrate when 50% H_2O_2 is used, the following parameters apply: $[S]_\infty/[S]_0 = 0.01$ and $\alpha = 17$ M. In the same way, a constant average value of $k_d \approx 2.5 \times 10^4$ s^{-1} may be assumed since the small amount of added water does not significantly modify $^1O_2$ lifetime. The insertion of all these values into eq 10 allows to calculate the maximum concentration of substrate that can be completely oxidized within the microemulsion B according to eq 25.

$$[S]_0 \leq \frac{0.86 k_r - 1.16 \times 10^5}{k_r + k_q} \qquad (25)$$

This inequality displays two limiting conditions for the complete oxidation of organic substrates: first, the concentration of substrate must always be less than 0.86 M even when very reactive compounds are oxidized; second, only substrates with sufficient reactivity ($k_r > 1.3 \times 10^5$ M^{-1} s^{-1}) can be completely oxidized. Equation 25 may be translated graphically by plotting $k_r/(k_r + k_q)$ *versus* $\log(k_r + k_q)$ for a number of fixed value of $[S]_0$ (Figure 4). The x axis (i.e., $\log(k_r + k_q)$) represents the overall reactivity of the substrates toward $^1O_2$. The y axis, namely, $k_r/(k_r + k_q)$, is equal to the fraction of chemical quenching of $^1O_2$ by S (i.e., the ratio between the $^1O_2$ concentration that chemically reacts with S and the total amount of $^1O_2$ that interacts with it).

The overall rate constants, namely, $k_r + k_q$, are known for many organic compounds, since they are readily measured by flash photolysis; whereas, the reported chemical rate constants k_r are quite scarce. Most of them have been compiled by

Wilkinson et al.[16] The values found in the literature for the substrates under study have been reported in Table 2. Thus, with the help of Figure 4, we can estimate the maximum concentration which may be completely oxidized within the microemulsion B for a given substrate. In fact, for several compounds (rubrene (**1**), 9,10-diphenylanthracene (**2**), 1,3-diphenylisobenzofuran (**3**), tetracyclone (**4**), and adamantyli-deneadamantane (**6**)), the predicted concentrations cannot be attained, since their solubility is the limiting factor rather than the reactivity. Thus, the microemulsion B is convenient to oxidize all of the sparingly soluble chemicals and, more generally, the substrates that are sufficiently reactive ($k_r > 10^6$ M^{-1} s^{-1}). However, this microemulsion is not suitable for concentrated solutions of substrates ($[S]_0 > 0.1$ M), since the low concentration of catalyst ($[MoO_4^{2-}] = 5$ mmol kg^{-1}) would lead to prohibitive reaction time ($\Delta \geq 2$ h).

Therefore, a microemulsion suitable for the oxidation of the readily soluble (α-terpinene (**5**), citronellol (**7**)) and the poorly reactive (diphenyl sulfide (**10**)) substrates must contain a high concentration of catalyst and be able to dissolve large amounts of hydrogen peroxide in order to complete the reaction within a reasonable time. For this purpose, the microemulsion A was selected, with a BuOH/SDS weight ratio equal to 1, because it leads to the largest microemulsion domain in the oil-rich region in the presence of highly concentrated aqueous molybdate (0.8 M). On the basis of the solubility of hydrogen peroxide in this medium ($V/V_0 = 0.2$), we may expect to be able to oxidize the substrates that are either scarcely reactive ($k_r > 9 \times 10^4$ M^{-1} s^{-1}) or highly concentrated ($\sim$1.7 M). However, in the later case, such a high amount of starting material may affect the stability of the microemulsion. In this case, a new phase diagram must be worked out by replacing pure methylene chloride by a solution of the substrate in this solvent. Thus, by resorting to the microemulsion A, we were able to carry out

the oxidation of the compounds **5**, **7**, **8**, and **9** up to 99% completion. Nevertheless, diphenyl sulfide (**10**) was only partially converted (40%) into the corresponding sulfone since this substrate is poorly reactive toward $^1O_2$ ($k_r + k_q = 8 \times 10^4$ M^{-1} s^{-1} in CHCl$_3$) and exhibits probably some physical quenching ($k_r/(k_r + k_q) < 1$).

Conclusions

Microemulsions have been designed for the preparative scale oxidation of hydrophobic substrates with the chemical source of singlet oxygen H_2O_2/MoO_4^{2-}. In view of the submicronic diameter of the water droplets in these microemulsions, the $^1O_2$ molecules generated within this aqueous phase diffuse freely into the continuous organic phase before deactivation and react with the substrate. Flash photolysis experiments reveal the microheterogeneity of the medium since the lifetime of $^1O_2$ is up to twice as long as the value expected by assuming that the components are homogeneously mixed. A kinetic model has been advanced for describing the behavior of $^1O_2$ toward organic substrates dissolved in the microemulsion. It was shown that only sufficiently reactive compounds ($k_r > 10^5$ M^{-1} s^{-1}) can be completely oxidized by this method. A variety of typical substrates have been employed, and a simple procedure to recover the product, the surfactant, and the catalyst has been developed.